POLITECNICO DI TORINO
Repository ISTITUZIONALE

Nonlinear and linearized vibration analysis of plates and shells subjected to compressive loading

Original
Nonlinear and linearized vibration analysis of plates and shells subjected to compressive loading / Azzara, R.; Carrera, E.; Pagani, A.. - In: INTERNATIONAL JOURNAL OF NON-LINEAR MECHANICS. - ISSN 0020-7462. - STAMPA. - 141:(2022), p. 103936. [10.1016/j.ijnonlinmec.2022.103936]

Availability:
This version is available at: 11583/2954496 since: 2022-03-05T10:13:54Z

Publisher:
Elsevier Ltd

Published
DOI:10.1016/j.ijnonlinmec.2022.103936

Terms of use:

This article is made available under terms and conditions as specified in the corresponding bibliographic description in the repository

Publisher copyright

(Article begins on next page)

25 April 2024

Nonlinear and linearized vibration analysis of plates and shells subjected to compressive loading

R. Azzara[1]*, E. Carrera[1,2]†, A. Pagani[1]‡

[1] Department of Mechanical and Aerospace Engineering, Politecnico di Torino
Corso Duca degli Abruzzi 24, 10129 Torino, Italy.
[2] Department of Mechanical Engineering, College of Engineering,
Prince Mohammad Bin Fahd University. Kingdom of Saudi Arabia.

Abstract: *The present work provides a numerical model for carrying out virtual Vibration Correlation Technique (VCT) for computing the buckling load, identifying the natural frequencies variation with progressive higher applied load, and providing an efficient means for the verification of the experimental VCT results. The presented nonlinear approach is based on the Carrera Unified Formulation (CUF). Since far nonlinear regimes are investigated, the full Green-Lagrange strain tensor is adopted. Furthermore, geometrical nonlinear equations are written in a total Lagrangian framework and solved with an opportune Newton-Raphson method. For a robustness assessment of the virtual VCT, different flat panel and shell structures are studied and compared with results found in the available literature. The results prove that the proposed approach provides results with an excellent correlation with the experimental ones, allowing to predict the buckling load and the natural frequencies variation in the nonlinear regime with high reliability.*

Keywords: Buckling; Natural frequencies; Vibration Correlation Technique; Carrera Unified Formulation; Two-dimensional (2D) model; Geometrical nonlinearity.

1 Introduction

Experimental campaigns continue to be essential for the design and validation of the methodologies of the new structures. However, studying the stability of structures subjected to compressive loads, it is noticeable how difficult it is to determine the buckling load by carrying out static tests experimentally. This complexity is due to the presence of imperfections in the specimens or to different boundary conditions, which have a remarkable influence on the critical load. Therefore, the possibility of carrying out nondestructive experimental tests for the prediction of the critical load is essential. In fact, robust and reliable nondestructive methods have been extensively studied for decades in order to minimize the time and cost of operations.

The first nondestructive method appeared in the early 1930s, intending to compute the buckling load of simple beam models using the Southwell method [1]. One of the most reliable nondestructive approaches adopted in the aerospace industry is the Vibration Correlation Technique (VCT) [2, 3]. This method calculates the buckling load and the equivalent boundary conditions by interpolating the natural frequencies of the structures for progressively increasing applied loads without reaching the point of instability. VCT has generally divided into two main groups: 1) to determine the in situ boundary condition; 2) to predict the buckling loads. The first experimental VCT investigations were data from the 1950s, with the studies conducted by Lurie [4], Meier [5] and Chu [6].

*PhD student. E-mail: rodolfo.azzara@polito.it
†Professor of Aerospace Structures and Aeroelasticity. E-mail: erasmo.carrera@polito.it
‡Associate professor. E-mail: alfonso.pagani@polito.it

The VCT is achieved by applying compression loads to the structures well below the calculated critical load and extrapolating the value of the buckling load for which the frequency tends to zero. Considering simple supports, the relation between frequencies squared and compressive loadings is totally linear. In this particular case, the vibration mode is identical to the buckling mode. Instead, for other constraints, important deviations from linearity can be significant. In addition, initial geometric imperfections have a noticeable effect on the critical load. Therefore, nonlinear studies are required to perform accurate analysis and verification of the results. Massonnet [7], for example, observed in his nonlinear studies on imperfect curved plates that the vibration frequency increases after the plate had buckled due to the nonlinear effect of post-buckling distortions. The defined variation in frequency slope as a load function could indicate another criterion for buckling prediction. In this context, several experiments were performed obtaining the same conclusions regarding the increase in frequencies after buckling [8, 9, 10]. An important literature review focused on the most important research on nonlinear vibrations in structures can be found in [11].

VCTs were applied to beams columns [12, 13, 14] for decades by reaching maturity in industrial applicability, whereas further improvements are still being developed for plates and shells. The applicability and verification of the VCT for computing the critical load for plate and shell structures is a vivid research area. The literature on this topic is vast. For instance, recent studies were presented by Abramovich [15], where the VCT was adopted to obtain the buckling loads of stiffened metallic and laminated curved panels. The same author summarized the current state-of-the-art of the VCT studies in [16]. A modified-VCT provided by Arbelo [17], based on the considerations made by Souza [18], was adopted by Skukis *et al.* [19] in order to capture the critical loads of unstiffened shell with circular cut-outs under compressive load. Singhtanadgid and Sukajit [20] derived from the differential governing equations the link between applied loadings and natural frequencies of plate structures. After that, the numerical determination of buckling loads was compared with the experimental solutions. The appropriateness of the VCT for buckling estimation in metallic shell structures under compressive loading was investigated by Skukis *et al.* [21]. A semi-analytical VCT formulation to have a direct prediction of critical loads of shells was provided by Jansen *et al.* [22]. Franzoni *et al.* [23] carried out experimental verification of the VCT robustness to investigate the buckling of laminated shell structures. The same author [24] presented an analytical and numerical verification of the VCT to derive the critical load of imperfection-sensitive metallic cylindrical structures. Readers are referred to the books of Singer *et al.* [2, 3] and Abramovich [25] for a detailed and complete description of the experimental setup and results.

The principal aim of this research is to present a numerical model for carrying out virtual VCT to compute the buckling load, to evaluate the natural frequencies variation with progressively increasing loadings, and to create an efficient means for the verification of the experimental VCT results, considering the geometrical nonlinear relations. The investigated structure is subjected to progressively higher applied loads, and for each state of equilibrium, on the deformed structure, the natural frequencies are calculated by solving a linearized eigenvalue problem, obtained from an analysis of the free vibration on the structure.

The presented nonlinear approach is formulated in the domain of the Carrera Unified Formulation (CUF) [26, 27]. The main advantage of CUF is that the structural model becomes an input of the analysis. In this way, no ad-hoc formulations are necessary to obtain refined models. According to CUF, all the theories of structures can be obtained as degenerated cases of an arbitrary expansion of the generalized unknowns. By adopting this procedure, the nonlinear governing equations and the relative finite element (FE) arrays of the two-dimensional (2D) theories are written in terms of Fundamental Nuclei (FNs). FNs represent the basic building blocks of the presented theory. Different engineering problems and fields have been analyzed employing the CUF [28, 29, 30, 31, 32, 33]. In this paper, this method is adopted to manage with vibrations.

This article is organized as follows: (i) some essential aspects regarding the CUF and the virtual VCT methodology used in this research are provided in the first Section 2; (ii) next, Section 3 discusses the numerical examples; (iii) finally, Section 4 reports the main conclusions.

2 Virtual Vibration Correlation Technique

2.1 Carrera Unified Formulation

In this article, the isotropic structures are modelled using refined 2D CUF models. Consider a 2D model, which is described in Fig. 1 using a Cartesian system (x,y,z) for plates and an orthogonal curvilinear system (α,β,z) for shells, where x, y and α, β denote the two in-plane directions and z is the through-the-thickness direction. The nonlinear problem is formulated in a total Lagrangian

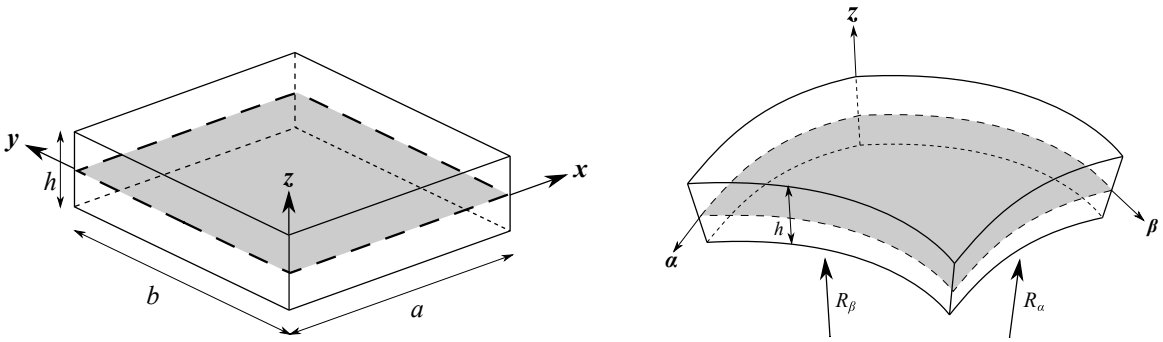

(a) (b)

Figure 1: Geometry and reference system of a generic (a) plate and (b) doubly-curved shell.

framework and the Green-Lagrange strain tensor $\boldsymbol{\epsilon}$ is considered. The displacement-strain relations are written as:

$$\boldsymbol{\epsilon} = \boldsymbol{\epsilon}_l + \boldsymbol{\epsilon}_{nl} = (\boldsymbol{b}_l + \boldsymbol{b}_{nl})\boldsymbol{u} \tag{1}$$

where the three-dimensional (3D) displacement, strain and stress vectors of a generic point within the structural domain of a shell are defined as follows:

$$\begin{aligned} \boldsymbol{u} &= \{\, u_\alpha,\ u_\beta,\ u_z \,\}^{\mathrm{T}} \\ \boldsymbol{\epsilon} &= \{\epsilon_{\alpha\alpha},\ \epsilon_{\beta\beta},\ \epsilon_{zz},\ \epsilon_{\alpha z},\ \epsilon_{\beta z},\ \epsilon_{\alpha\beta}\}^{\mathrm{T}} \\ \boldsymbol{\sigma} &= \{\sigma_{\alpha\alpha},\ \sigma_{\beta\beta},\ \sigma_{zz},\ \sigma_{\alpha z},\ \sigma_{\beta z},\ \sigma_{\alpha\beta}\}^{\mathrm{T}} \end{aligned} \tag{2}$$

Although derivation is carried out for shells in the following sections, it should be underlined that similar relations hold for plates. In Eq. 1, $\boldsymbol{b}_l$ and $\boldsymbol{b}_{nl}$ represent linear and nonlinear differential operators. Readers can be found the complete form of these matrices in [34].

According to CUF, the 3D displacement field in the dynamic case $\boldsymbol{u}(\alpha, \beta, z; t)$ is defined as an arbitrary through-the-thickness expansion of the in-plane variables:

$$\boldsymbol{u}(\alpha, \beta, z; t) = F_\tau(z)\boldsymbol{u}_\tau(\alpha, \beta; t) \qquad \tau = 1, ..., M \tag{3}$$

in which $\boldsymbol{u}_\tau(\alpha, \beta; t)$ is the generalized in-plane displacement vector, F_τ represent the expansion functions of the thickness coordinate z, M is the order of expansion in the thickness direction and t denotes time. Readers are referred to [27] for a full explanation about the mathematical derivation of the 2D FE formulation in the domain of CUF. In this article, Lagrange polynomials (LE) are adopted for the expansion functions F_τ. Note that the acronym LEN, considered in this article, denotes the LE of order N assumed in the z direction.

The finite element method (FEM) is used to approximate the in-plane generalized displacement vector employing the shape function $N_i(\alpha, \beta)$.

$$\boldsymbol{u}_\tau(\alpha, \beta; t) = N_i(\alpha, \beta)\boldsymbol{q}_{\tau i}(t) \qquad i = 1, 2, ..., N_n \tag{4}$$

in which $\boldsymbol{q}_{\tau i}$ represents the vector of the unknown nodal variables, N_n denotes the number of nodes per element and the i stands for summation. In particular, the classical 2D nine-node quadratic (Q9) FE will be assumed in the following analyses as the shape function in the $\alpha - \beta$ plane, see Fig. 2.

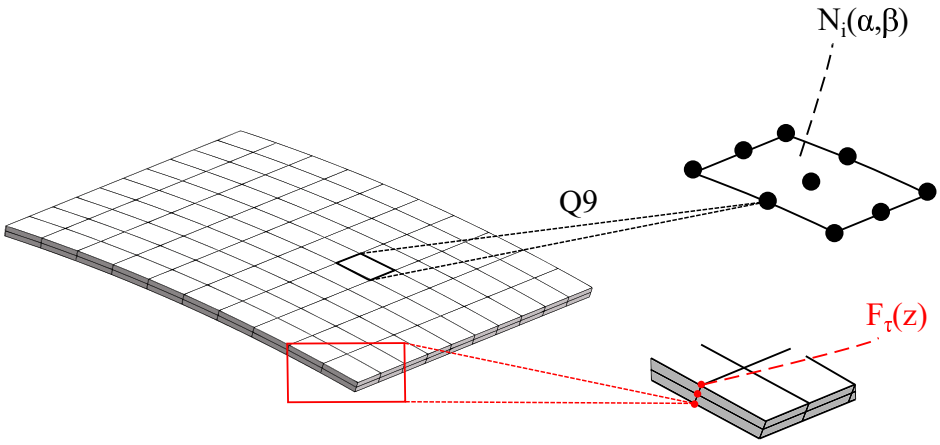

Figure 2: The 2D model approximations of a typical shell structure.

By having the strain ($\boldsymbol{\epsilon}$) and considering the CUF (Eq. 3) and FEM (Eq. 4) relations into Eq. 1, the strain vector can be formulated in algebric form as:

$$\boldsymbol{\epsilon} = (\boldsymbol{B}_l^{\tau i} + \boldsymbol{B}_{nl}^{\tau i})\boldsymbol{q}_{\tau i} \tag{5}$$

where $\boldsymbol{B}_l^{\tau i} = \boldsymbol{b}_l(F_\tau N_i)$ and $\boldsymbol{B}_{nl}^{\tau i} = \boldsymbol{b}_{nl}(F_\tau N_i)$. These linear and nonlinear matrices can be found in [35].

2.2 Nonlinear free vibration of structures

Vibration analysis is briefly introduced in this section. For this purpose, the virtual variation of the strain energy is formulated to derive the secant stiffness matrix ($\boldsymbol{K}_S$). Namely:

$$\begin{aligned}\delta L_{int} &= \delta \boldsymbol{q}_{sj}^{\mathrm{T}} \boldsymbol{K}_0^{ij\tau s} \boldsymbol{q}_{\tau i} + \delta \boldsymbol{q}_{sj}^{\mathrm{T}} \boldsymbol{K}_{lnl}^{ij\tau s} \boldsymbol{q}_{\tau i} + \delta \boldsymbol{q}_{sj}^{\mathrm{T}} \boldsymbol{K}_{nll}^{ij\tau s} \boldsymbol{q}_{\tau i} + \delta \boldsymbol{q}_{sj}^{\mathrm{T}} \boldsymbol{K}_{nlnl}^{ij\tau s} \boldsymbol{q}_{\tau i} \\ &= \delta \boldsymbol{q}_{sj}^{\mathrm{T}} \boldsymbol{K}_S^{ij\tau s} \boldsymbol{q}_{\tau i}\end{aligned} \tag{6}$$

where $\boldsymbol{K}_0^{ij\tau s}$ is the linear contribution of $\boldsymbol{K}_S$ and $\boldsymbol{K}_{lnl}^{ij\tau s}$, $\boldsymbol{K}_{nll}^{ij\tau s}$ and $\boldsymbol{K}_{nlnl}^{ij\tau s}$ indicate the nonlinear contributions of different orders, respectively. These components are written in the form of CUF 3×3 Fundamental Nuclei (FNs). For clarity, FNs represent the basic building blocks of the presented theory. The FN is independent of the theory approximation and can be expanded against F_τ approximation ($\tau, s = 1, ..., M$) and N_i shape functions ($i, j = 1, ..., N_n$) to obtain the final stiffness matrix of any high-order model. Readers are referred to [27] to see how it is possible to build a matrix of the node, of the element and, finally, the global stiffness matrix $\boldsymbol{K}_S$ by exploiting the FNs.

By employing the principle of virtual work, the virtual variations of internal and external work, where the latter is not reported here for the sake of brevity, are considered to obtain the system of nonlinear equilibrium equations.

$$\boldsymbol{K}_S^{ij\tau s} \boldsymbol{q}_{\tau i} = \boldsymbol{p}_{sj} \tag{7}$$

$\boldsymbol{K}_S^{ij\tau s}$ and $\boldsymbol{p}_{sj}$ are the FNs of the secant stiffness matrix and the vector of the nodal loadings, respectively. This set of equations is solved using the Newton-Raphson method based on the arc-length approach [36, 37].

Similarly, the FNs of the mass matrix are obtained from the virtual variation of the inertial loads:

$$\delta L_{ine} = \delta \boldsymbol{q}_{sj}^{\mathrm{T}} \boldsymbol{M}^{ij\tau s} \ddot{\boldsymbol{q}}_{\tau i} \tag{8}$$

in which $\boldsymbol{M}^{ij\tau s}$ represents the FN of the mass matrix and $\ddot{\boldsymbol{q}}_{\tau i}$ indicates the nodal acceleration vector; the dot stands for time derivative. The derivation of FN of the mass matrix is provided in [27].

Because the modal behaviour of a structure is not a property of the geometric and mechanical characteristics, but it is a property of the state of equilibrium, eigenfrequencies and eigenmodes may suffer abrupt aberrations in deep nonlinear regimes. To investigate this aspect, the vibration analysis is carried out around a linearized (*non-trivial*) equilibrium state along the nonlinear path. By linearizing the virtual variation of the nonlinear strain energy, the tangent stiffness matrix ($\boldsymbol{K}_T$) is introduced.

$$\begin{aligned}\delta(\delta L_{int} + \delta L_{ine} - \delta L_{ext}) = \delta\boldsymbol{q}_{sj}^{\mathrm{T}}(\boldsymbol{K}_0^{ij\tau s} + \boldsymbol{K}_{T1}^{ij\tau s})\delta\boldsymbol{q}_{\tau i} + \delta\boldsymbol{q}_{sj}^{\mathrm{T}}\boldsymbol{K}_{\sigma}^{ij\tau s}\delta\boldsymbol{q}_{\tau i} + \delta\boldsymbol{q}_{sj}^{\mathrm{T}}\boldsymbol{M}^{ij\tau s}\delta\ddot{\boldsymbol{q}}_{\tau i} = \\ = \delta\boldsymbol{q}_{sj}^{\mathrm{T}}\boldsymbol{K}_T^{ij\tau s}\delta\boldsymbol{q}_{\tau i} + \delta\boldsymbol{q}_{sj}^{\mathrm{T}}\boldsymbol{M}^{ij\tau s}\delta\ddot{\boldsymbol{q}}_{\tau i} = 0\end{aligned} \tag{9}$$

In deriving Eq. 9, the mass matrix is assumed linear and $\delta^2 L_{ext} = 0$ (loading is conservative). $\boldsymbol{K}_T^{ij\tau s}$ represents the FN of the tangent stiffness matrix, $\boldsymbol{K}_0^{ij\tau s}$ indicates the linear component of $\boldsymbol{K}_T$, $\boldsymbol{K}_{T1}^{ij\tau s} = 2\boldsymbol{K}_{lnl}^{ij\tau s} + \boldsymbol{K}_{nll}^{ij\tau s} + 2\boldsymbol{K}_{nlnl}^{ij\tau s}$ denotes the nonlinear contribution, and $\boldsymbol{K}_{\sigma}^{ij\tau s}$ is the so-called geometric stiffness, which is a function of the linear ($\boldsymbol{K}_{\sigma_l}$) and nonlinear ($\boldsymbol{K}_{\sigma_{nl}}$) pre-stress state, where:

$$\begin{aligned}\boldsymbol{\sigma} &= \boldsymbol{C}(\boldsymbol{\epsilon}_l + \boldsymbol{\epsilon}_{nl}) \\ \boldsymbol{\sigma}_l &= \boldsymbol{C}\boldsymbol{\epsilon}_l\end{aligned} \tag{10}$$

and $\boldsymbol{C}$ is the material elastic matrix. The full expressions of these matrices for plates and shells can be found in [35].

Displacement variation in Eq. 9 are small so that harmonic vibration can be assumed and the system solved as a linear eigenvalue problem. In summary, the virtual VCT analysis to investigate the vibration around nonlinear equilibrium states can be carried out as follows:

- First, the static geometrical nonlinear problem is solved using the Newton-Raphson method based on the arc-length approach.
- Once the nonlinear equilibrium curve is computed, the tangent stiffness matrix is obtained in each states of interest, see Fig. 3.

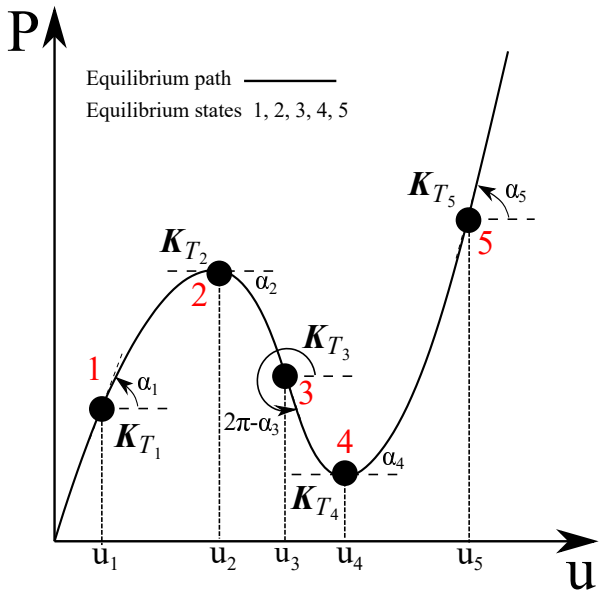

Figure 3: $\boldsymbol{K}_T$ for representative states of equilibrium of a generic nonlinear equilibrium curve.

- Then, by considering the incremental linearized equilibrium condition of Eq. 9 and assuming harmonic motion around non-trivial equilibrium states,

$$\begin{aligned} \delta \boldsymbol{q}_{\tau i}(t) &= \delta \widetilde{\boldsymbol{q}}_{\tau i} e^{i\omega t} \\ \delta \ddot{\boldsymbol{q}}_{\tau i}(t) &= -\omega^2 \delta \widetilde{\boldsymbol{q}}_{\tau i} e^{i\omega t} \end{aligned} \tag{11}$$

  the equations of motion is simplified into a linear eigenvalues problem from which it is possible to evaluate natural frequencies and mode shapes:

$$(\boldsymbol{K}_T^{ij\tau s} - \omega^2 \boldsymbol{M}^{ij\tau s}) \delta \widetilde{\boldsymbol{q}}_{\tau i} = 0 \tag{12}$$

  where ω represents the natural frequency and $\delta \widetilde{\boldsymbol{q}}_{\tau i}$ is the eigenvector.

- For the sake of clarity, it is important to underline how the nonlinear vibrations exhibit low amplitudes; consequently, it is legitimate to use a linearization around the state of equilibrium for the resolution of the problem.

Typically, a resolution based on a linear approach is adopted in most works in the literature. For this reason, the comparison between linear and nonlinear approaches is emphasized in this work, showing the need to adopt a full nonlinear formulation to perform accurate analyzes.

By performing the linearization around *trivial* equilibrium state, the stiffness matrix is given by:

$$\boldsymbol{K}_T \cong \boldsymbol{K}_0 + \lambda \boldsymbol{K}_{\sigma_l} \tag{13}$$

where λ is the load factor.

3 Numerical examples

This section examines representative benchmark problems, emphasizing the capabilities of this proposed approach to perform virtual VCT to compute the critical load of structures, to evaluate the natural frequencies variation with progressively higher loadings, and to provide a verification of the experimental VCT results. For this purpose, flat panel and shell structures were investigated and compared with the available literature results.

3.1 Flat panels

Two different aluminium plates subjected to compressive load are considered as the first analysis case. In particular, for the plate 2 also traction load was considered. These benchmark cases have the following geometrical characteristics: a) *plate 1*: width (a) is 355 mm, length (b) equal to 355 mm and the thickness (t) is 2 mm; b) *plate 2*: a=b= 200 mm and t= 1.955 mm. The boundary conditions of these two plate structures are shown in Fig. 4. In particular, these constraints are clamped-clamped-simply supported-simply supported (CCSS) for plate 1 and clamped-clamped-clamped-free (CCCF) for plate 2. Both structures have the following material properties, E= 70 GPa, ν= 0.33 and ρ= 2780 kg/m^3.

First, to carry out an accurate investigation, a convergence analysis is performed. Consequently, the convergent model for these aluminium plate structures is reached employing at least 10×10Q9 for the in-plane mesh approximation and only one LE2 in the thickness direction. The convergence analysis is not shown here for the sake of brevity. Nevertheless, convergence performance of the proposed finite elements can be appreciated in [38].

Figure 5 shows the equilibrium curves of the aluminium plates under compressive load. In the case of nonlinear analysis, a defect load applied in the center of the plates, d= 0.01 N, was used. First, the variation of natural frequencies versus compressive loading via trivial linearized solution is illustrated in Fig. 6. In particular, for plate 2, both tensile and compressive loads are considered.

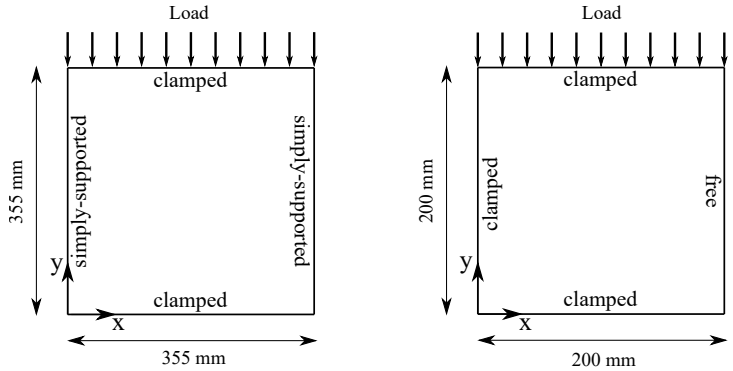

(a) Plate 1 (b) Plate 2

Figure 4: Geometry and boundary conditions of the aluminium plates.

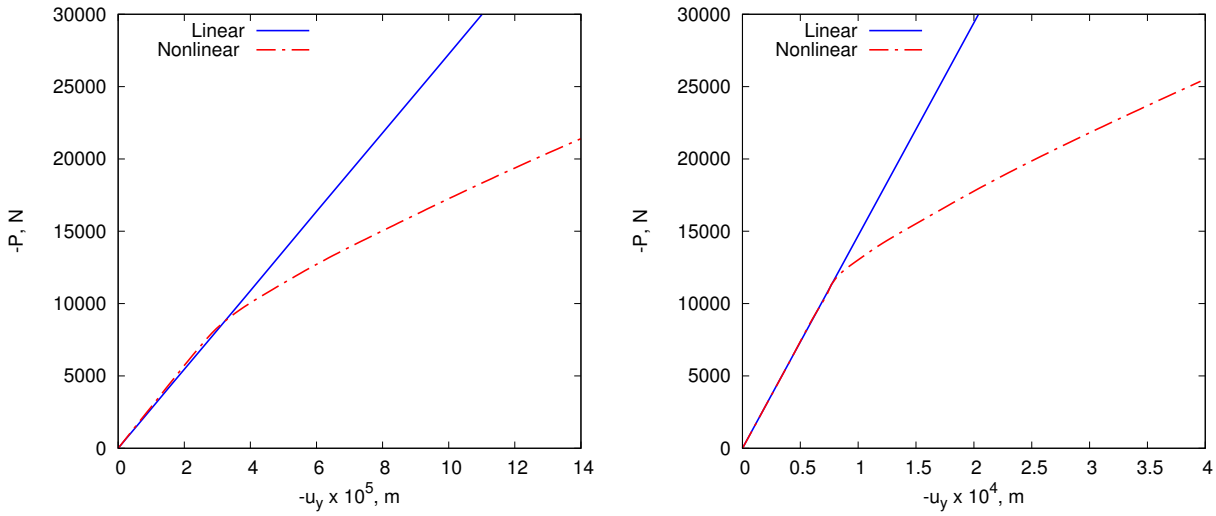

(a) Plate 1 (b) Plate 2

Figure 5: Linear and nonlinear load-deflection curves. Aluminium plates subjected to compressive load.

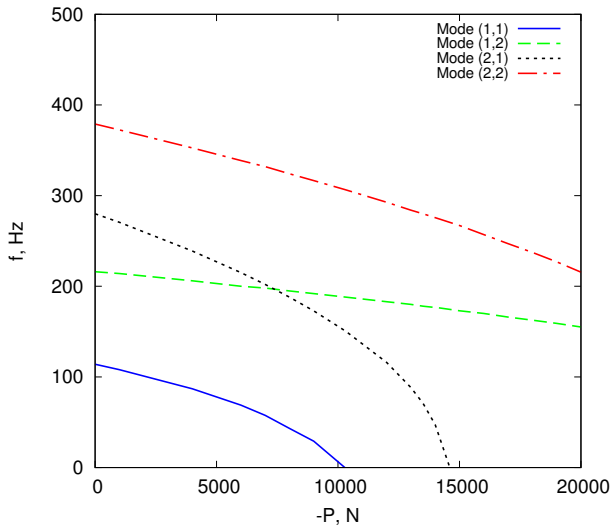

(a) Plate 1

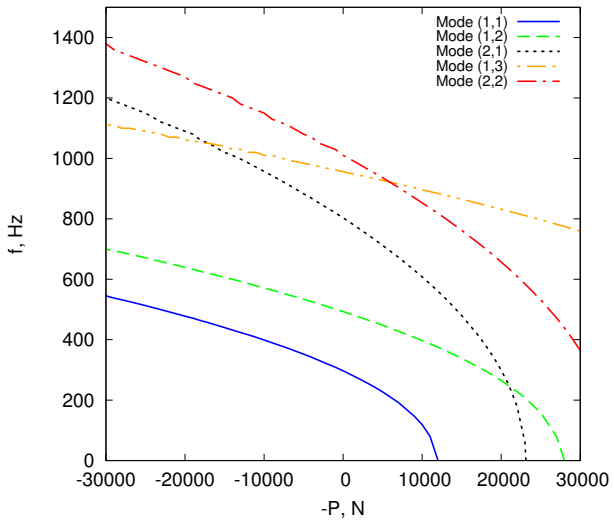

(b) Plate 2

Figure 6: Natural frequencies variation versus compressive loading via trivial linearized solution for the aluminium plates.

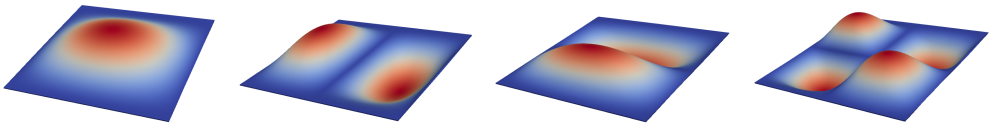

(a) Mode (1,1) (b) Mode (1,2) (c) Mode (2,1) (d) Mode (2,2)

Figure 7: Characteristics first four free vibration mode shapes for the aluminium plate 1.

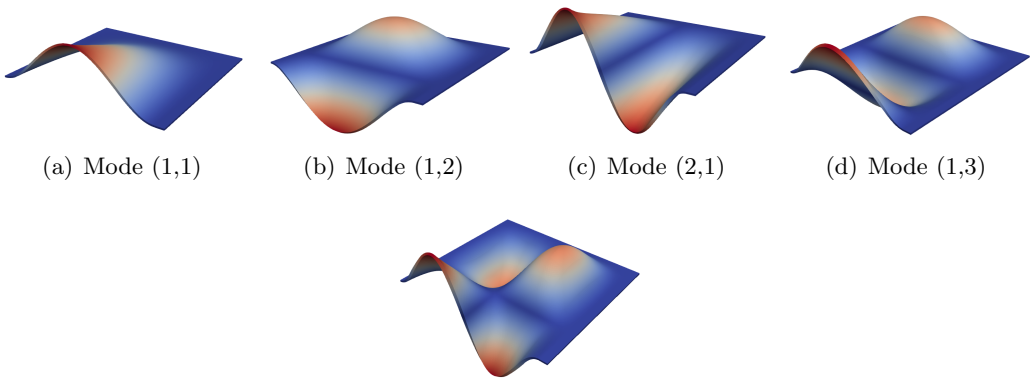

(a) Mode (1,1) (b) Mode (1,2) (c) Mode (2,1) (d) Mode (1,3)

(e) Mode (2,2)

Figure 8: Characteristics first five free vibration mode shapes for the aluminium plate 2.

The characteristics first four vibration mode shapes of the aluminium plate 1 and the first five vibration mode shapes of the aluminium plate 2 at P= 0 N are provided in Fig. 7 and Fig. 8. Instead, the natural frequencies variation versus compressive loading via full nonlinear solution is represented in Fig. 9.

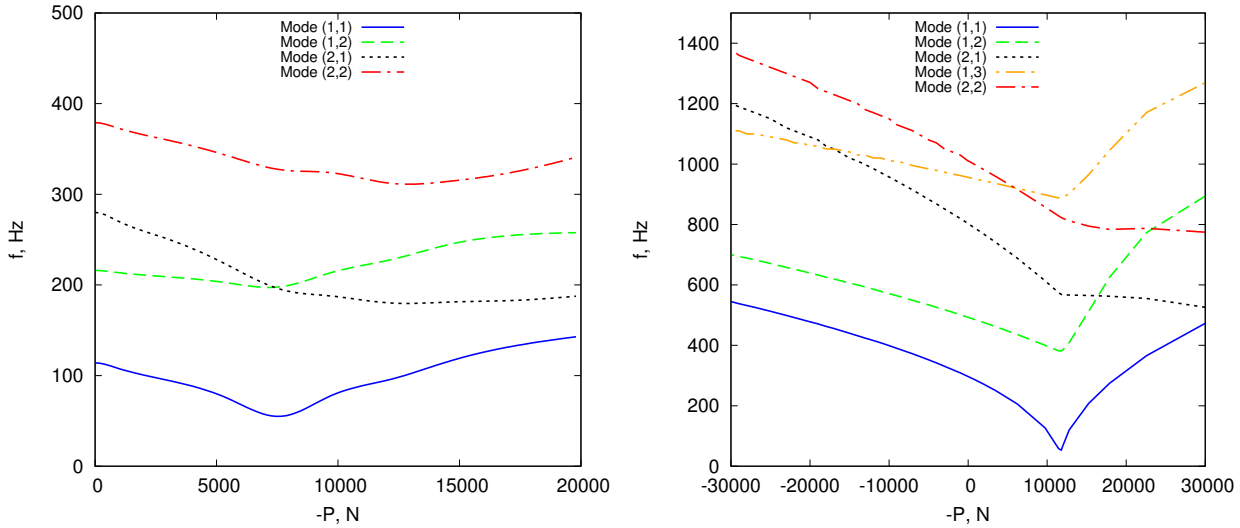

(a) Plate 1 (b) Plate 2

Figure 9: Natural frequencies variation versus compressive loading via full nonlinear solution. Aluminium flat panels.

Table 1 shows the aluminum plates' buckling load values compared to experimental results. For clarity, the simulation results come from a simple linearized buckling analysis, in which the tangent stiffness is approximated as the sum of the linear matrix and the geometric stiffness resulting from linear stress state. Discrepancies between the numerical solution based on the current approach and the experimental buckling load are described as a percentage difference. In particular, the

Model	Plate 1		Plate 2	
	Buckling Load	%Diff	Buckling Load	%Diff
Present Numerical solution	10.28	2.80	11.85	1.82
Exp. Measurement [17, 20]	10.00	-	12.07	-

Table 1: The linearized bucking loads in [kN] of aluminium plates.

discrepancy of the measured critical load employing the proposed methodology is minimal compared to experimental solutions.

Figure 10 illustrates the comparison between the natural frequencies variation for progressively increasing loading obtained via trivial linearized solution, via full nonlinear solution and the experimental results. The results provided in Fig. 10 show that the approach based on the trivial linearized solution allows one to evaluate the frequency variation of these benchmark cases at lower levels of the compressive load with accuracy. The deviation of the linear results from the nonlinear and experimental ones becomes remarkable for higher compressive load levels. In particular, considering the trivial linearized approach, it can be noted that the frequency of the first vibration mode tends to zero at the buckling load value. On the other hand, the nonlinear and experimental solutions exhibited a different behaviour. In detail, the first vibration mode reaches a minimum value near the critical load, and after the buckling, the frequencies increase. This definite change in the slope of the frequencies represents a criterion for the buckling prediction. This difference

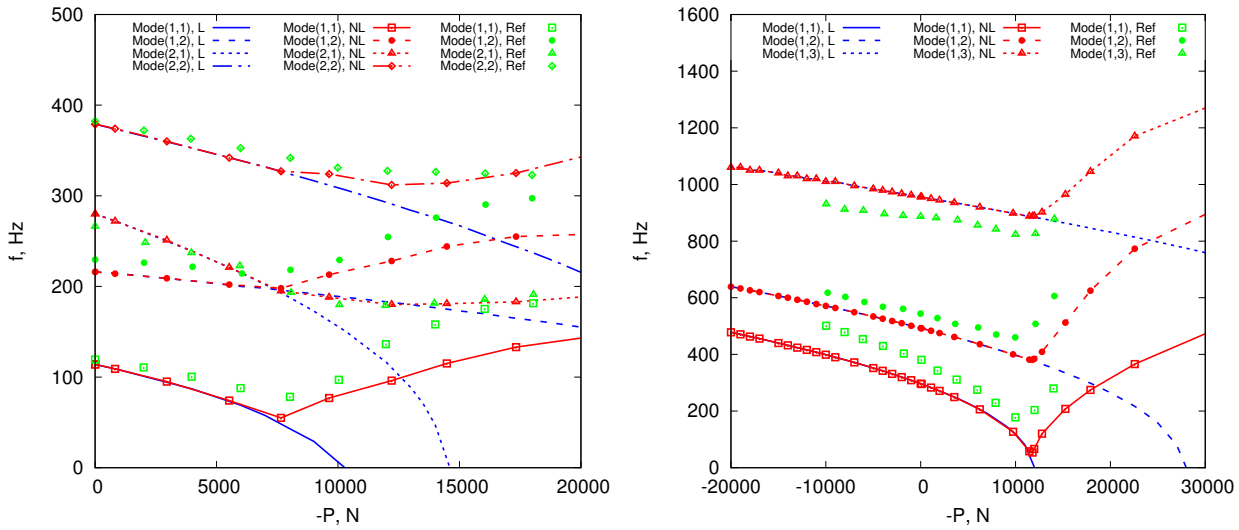

(a) Plate 1 [17] (b) Plate 2 [20]

Figure 10: Comparison between the natural frequencies variation versus compressive loading via trivial linearized solution, via full nonlinear solution and experimental results for aluminium plates.

between trivial linearized solution and full nonlinear approach is due to the nonlinear effects of the post-buckling. The results obtained using the proposed nonlinear virtual VCT approach show an excellent correlation with the experimental ones, allowing to calculate the critical load and to evaluate the natural frequencies variation in nonlinear regime with high reliability. The small discrepancies between the numerical and experimental solutions are probably attributed to variations between the actual boundary conditions adopted during the test and the numerical constraints and initial geometric imperfections.

3.2 Curved panel

Different curved panels subjected to compressive load are analyzed as the second analysis case. The investigated models have the following geometric data: L= 355 mm, a= 355 mm, t= 2 mm. The representation of the curved panel with R/a= 5 is illustrated in Fig. 11. Regarding the boundary conditions, the constraints are the same considered for the plate 1 in the previous case. The material properties for these curved panels are: E= 70 GPa, ν= 0.33 and ρ= 2780 kg/m^3. The convergent model for these curved panel structures is reached employing 10×10Q9 for the in-plane mesh approximation and only one LE2 in the thickness direction.

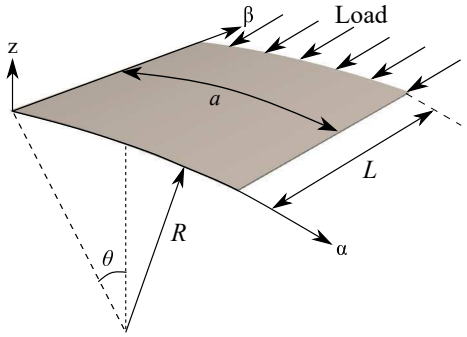

Figure 11: Curved panel with R/a= 5 subjected to compressive load.

The nonlinear quasi-static analysis has been performed for different values of R/a to evaluate the effect of the curvature. In contrast, VCT is only shown for the case R/a= 5 for the sake of brevity.

Figure 12a depicts the quasi-static equilibrium curves for the investigated metallic curved panels considering different R/a values. In detail, the equilibrium path of the curved panel case with R/a= 5 with some of the most relevant deformed configurations is reported in Fig. 12b. For different

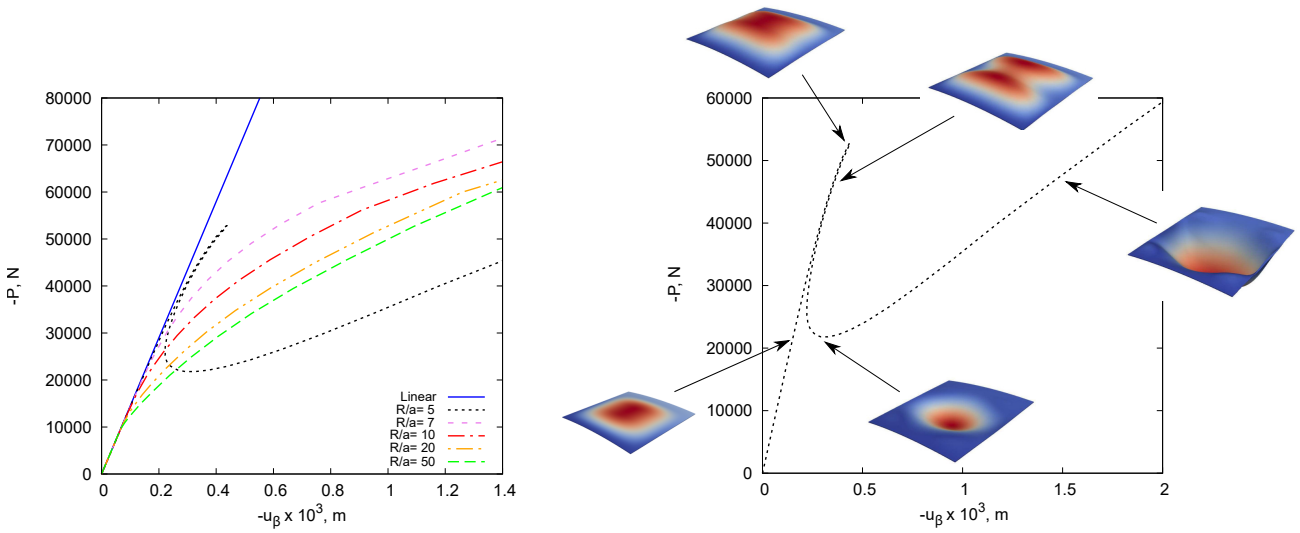

Figure 12: Equilibrium curve of the curved panels subjected to compressive load. (a) Different curvatures; (b) R/a= 5.

states of interest, the trend of the first ten natural frequencies with respect to the progressive load by means of the trivial linearized solution is provided in Fig. 13a. Instead, the natural frequency variation of mode 1 versus compressive loading via full nonlinear solution is depicted in Fig. 13b. It can be observed that considering the nonlinearity, the trend of the natural frequencies is very

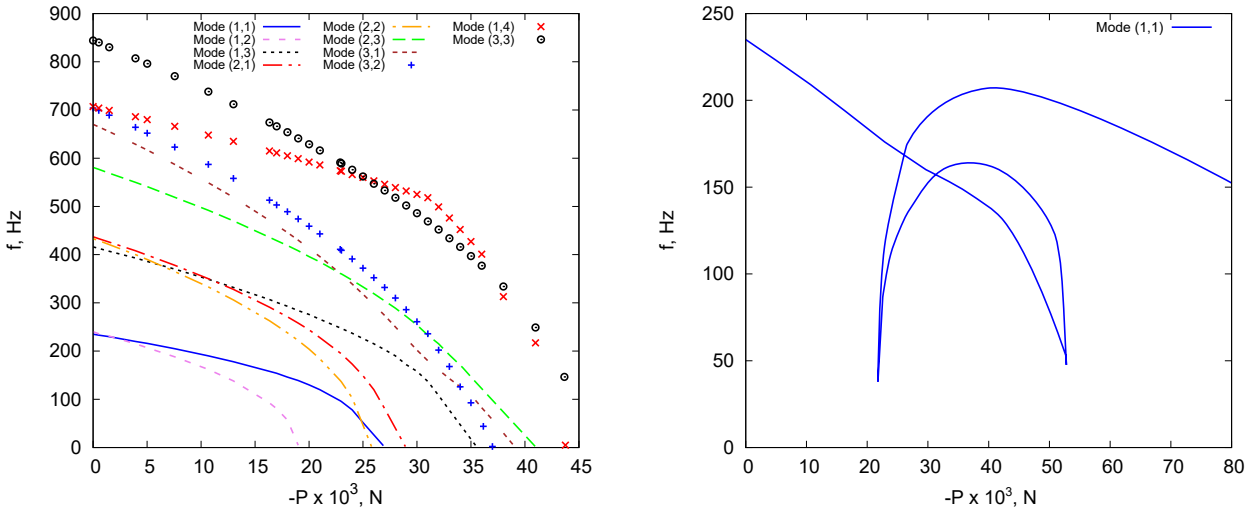

Figure 13: Natural frequency variation versus compressive loading via (a) trivial linearized solution and (b) full nonlinear solution. Curved panel with R/a= 5.

complex. The nonlinear variation of the natural frequencies was divided into three parts, Fig. 14, to plot more modes and have a better and clearer representation. The characteristics first ten vibration mode shapes of the curved panel with R/a= 5 at P= 0 N are provided in Fig. 15. As a result, it is possible to evaluate the complex trend of the natural frequencies with respect to the higher

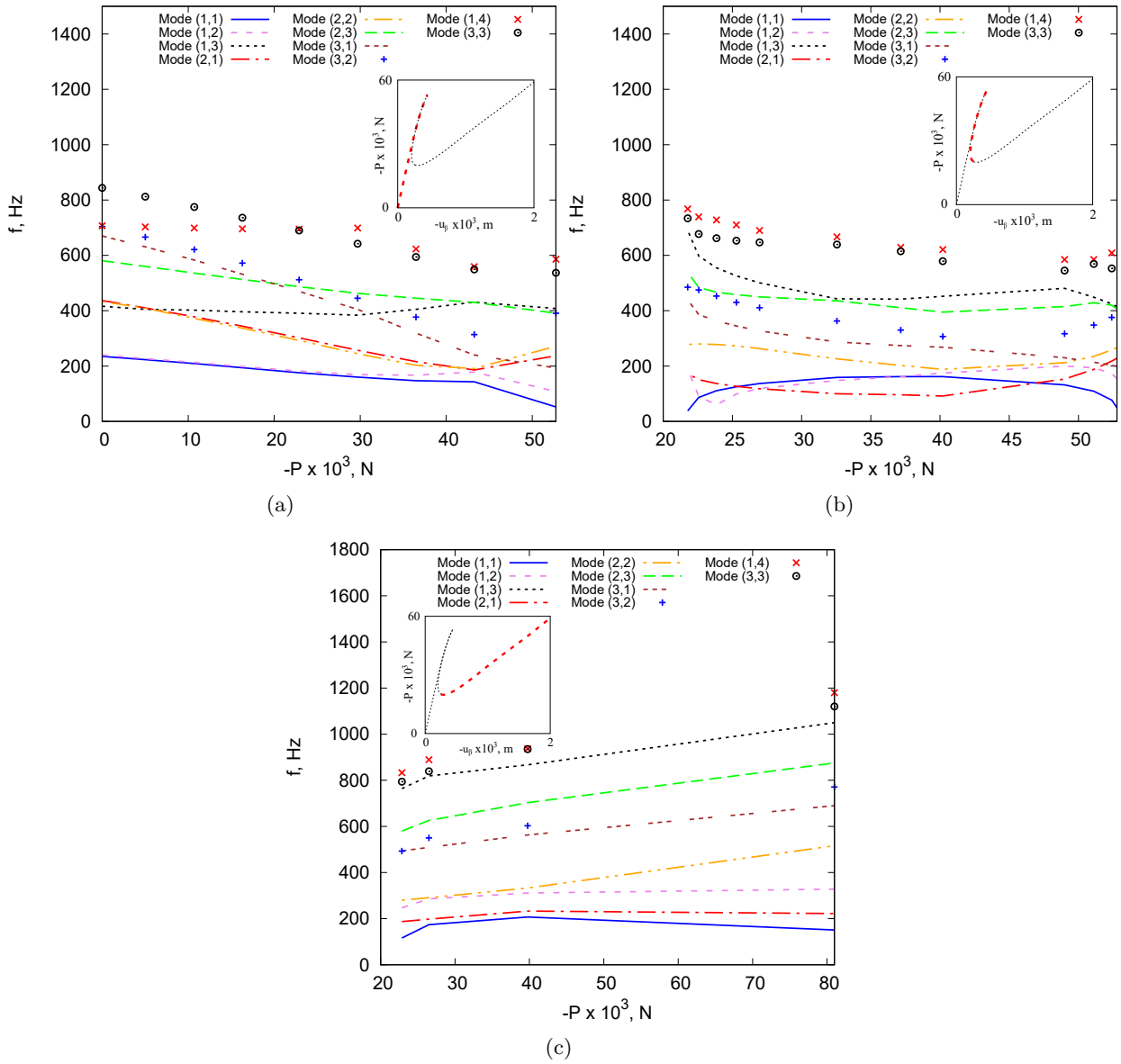

Figure 14: Nonlinear variation of the natural frequencies all along the quasi-static equilibrium path. Curved panel with R/a= 5.

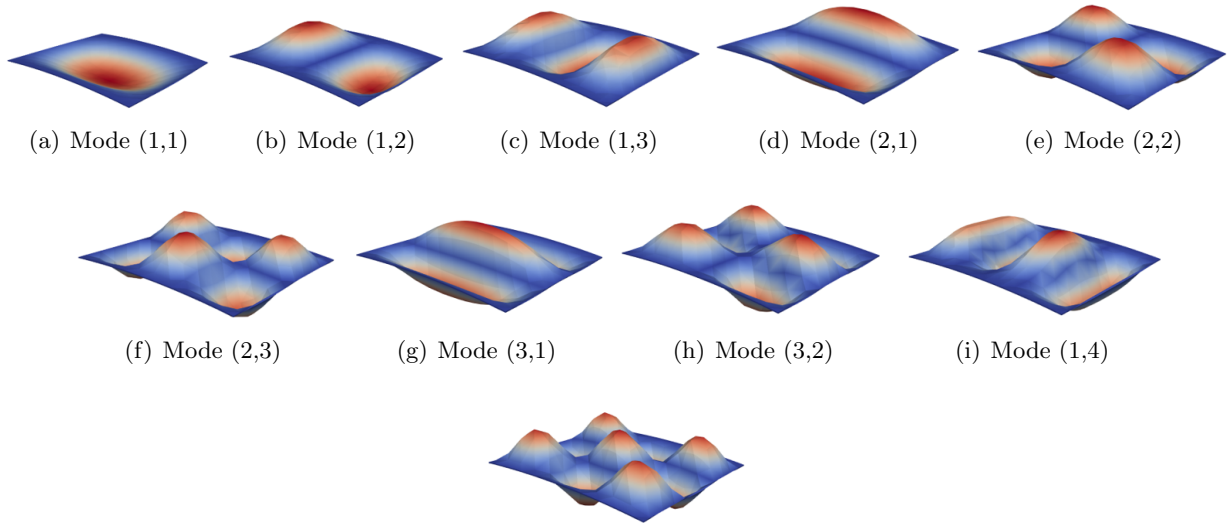

(a) Mode (1,1) (b) Mode (1,2) (c) Mode (1,3) (d) Mode (2,1) (e) Mode (2,2)

(f) Mode (2,3) (g) Mode (3,1) (h) Mode (3,2) (i) Mode (1,4)

(j) Mode (3,3)

Figure 15: Characteristics first ten free vibration mode shapes for the curved panel with R/a= 5.

progressive compressive loadings and to predict the linear and nonlinear buckling load by performing a nonlinear study.

4 Conclusions

The present paper provides a numerical methodology of the Vibration Correlation Technique (VCT) for metallic plates and shells, which represents one of the most employed nondestructive methods to evaluate the critical load of different aerospace structures. This method allows to determine the buckling load of structures by interpolating the natural frequencies for progressive higher loadings without reaching the instability point. The proposed method aims to provide a novel virtual VCT approach capable of predicting the buckling load, characterizing the natural frequencies' variation, and having an efficient means to verify the experimental VCT results. The analyses on flat panel and shell structures conducted in the domain of the Carrera Unified Formulation (CUF) and compared with the results found in the available VCT literature have demonstrated that this nonlinear approach is able to obtain results with high reliability and provide reasonable confidence for future applications in this topic. In particular, future works will concern the virtual VCT analysis of unstiffened and stiffened isotropic and composite plates and shells and of variable-angle-tow (VAT) composite structures.

References

[1] R.V. Southwell. On the analysis of experimental observations in problems of elastic stability. In *Proceedings of the Royal Society of London. Series A, Containing Papers of a Mathematical and Physical Character*, volume 135, pages 601–616. The Royal Society London, 1932.

[2] J. Singer, J. Arbocz, and T. Weller. *Buckling Experiments: Experimental Methods in Buckling of Thin-Walled Structures, Vol.1: Basic Concepts, Columns, Beams and Plate*. John Wiley & Sons, Inc., New York, USA, 1998.

[3] J. Singer, J. Arbocz, and T. Weller. *Buckling Experiments: Experimental Methods in Buckling of Thin-Walled Structures, Vol.2: Shells, Built-up Structures and Additional Topics*. John Wiley & Sons, Inc., New York, USA, 2002.

[4] H. Lurie. Lateral vibrations as related to structural stability. *Journal of Applied Mechanics, ASME*, 19:195–204, 1952.

[5] J.H. Meier. The determination of the critical load of a column or stiffened panel in compression by the vibration method. In *Proceeding of the Society for Experimental Stress analysis*, volume 11, 1953.

[6] T.H. Chu. *Determination of buckling loads by frequency measurements.* PhD thesis, California Institute of Technology, 1949.

[7] C. Massonnet. Le voilement des plaques planes sollicitées dans leur plan. *Final Report of the Third Congress of the International Association for Bridge and Structural Engineering*, pages 291–300, 1948.

[8] J.E.M. Jubb, I.G. Phillips, and H. Becker. Interrelation of structural stability, stiffness, residual stress and natural frequency. *Journal of Sound and Vibration*, 39(1):121–134, 1975.

[9] S. Ilanko and S.M. Dickinson. The vibration and post-buckling of geometrically imperfect, simply supported, rectangular plates under uni-axial loading, Part I: Theoretical approach. *Journal of Sound and Vibration*, 118(2):313–336, 1987.

[10] S. Ilanko and S.M. Dickinson. The vibration and post-buckling of geometrically imperfect, simply supported, rectangular plates under uni-axial loading, Part II: Experimental investigations. *Journal of Sound and Vibration*, 118(2):317–351, 1987.

[11] F. Moussaoui and R. Benamar. Non-linear vibrations of shell-type structures: a review with bibliography. *Journal of Sound and Vibration*, 255(1):161–184, 2002.

[12] R.H. Plaut and L.N. Virgin. Use of frequency data to predict buckling. *Journal of Engineering Mechanics*, 116(10):2330–2335, 1990.

[13] L.N. Virgin and R.H. Plaut. Axial load effects on the frequency response of a clamped beam. In *Proceeding of 21st IMAC Conference and Exposition on Structural Dynamics*, Kissimmee, Florida, USA, 2003.

[14] T.A. Alexander. The relationship between the buckling load factor and the fundamental frequency of a structure. In *Structures Congress 2005: Metropolis and Beyond*, pages 1–17, New York, USA, 2005.

[15] H. Abramovich, D. Govich, and A. Grunwald. Buckling prediction of panels using the vibration correlation technique. *Progress in Aerospace Sciences*, 78:62–73, 2015.

[16] H. Abramovich. The Vibration Correlation Technique - a reliable nondestructive method to predict buckling loads of thin walled structures. *Thin-Walled Structures*, page 107308, 2020.

[17] M.A. Arbelo, S.F.M. de Almeida, M.V. Donadon, S.R. Rett, R. Degenhardt, S.G.P. Castro, K. Kalnins, and O. Ozoliņš. Vibration Correlation Technique for the estimation of real boundary conditions and buckling load of unstiffened plates and cylindrical shells. *Thin-Walled Structures*, 79:119–128, 2014.

[18] M.A. Souza and L.M.B. Assaid. A new technique for the prediction of buckling loads from nondestructive vibration tests. *Experimental Mechanics*, 31(2):93–97, 1991.

[19] E. Skukis, K. Kalnins, and O. Ozolins. Application of Vibration Correlation Technique for open hole cylinders. In *Proceedings pf the 5th International Conference on Nonlinear Dynamics*, Kharkov, Ukraine, 2016.

[20] P. Singhatanadgid and P. Sukajit. Determination of buckling load of rectangular plates using measured vibration data. In *ICEM 2008: International Conference on Experimental Mechanics 2008*, volume 7375, page 73753Z. International Society for Optics and Photonics, 2009.

[21] E. Skukis, O. Ozolins, J. Andersons, K. Kalnins, and M.A. Arbelo. Applicability of the Vibration Correlation Technique for estimation of the buckling load in axial compression of cylindrical isotropic shells with and without circular cutouts. *Shock and Vibration*, 2017, 2017.

[22] E. Jansen, H. Abramovich, and R. Rolfes. The direct prediction of buckling loads of shells under axial compression using VCT-towards an upgraded approach. In *29th Congress on the International Council of the Aeronutical Science*, pages 1–9, 2014.

[23] F. Franzoni, F. Odermann, E. Lanbans, C. Bisagni, M.A. Arbelo, and R. Degenhardt. Experimental validation of the Vibration Correlation Technique robustness to predict buckling of unstiffened composite cylindrical shells. *Composite Structures*, 224:111107, 2019.

[24] F. Franzoni, R. Degenhardt, J. Albus, and M.A. Arbelo. Vibration Correlation Technique for predicting the buckling load of imperfection-sensitive isotropic cylindrical shells: An analytical and numerical verification. *Thin-Walled Structures*, 140:236–247, 2019.

[25] H. Abramovich. *Stability and vibrations of thin-walled composite structures*. Woodhead Publishing, 2017.

[26] E. Carrera, G. Giunta, and M. Petrolo. *Beam Structures: Classical and Advanced Theories*. John Wiley & Sons, 2011.

[27] E. Carrera, M. Cinefra, M. Petrolo, and E. Zappino. *Finite element analysis of structures through unified formulation*. John Wiley & Sons, 2014.

[28] E. Carrera, M. Petrolo, and A. Varello. Advanced beam formulations for free vibration analysis of conventional and joined wings. *Journal of Aerospace Engineering*, 25(2):282–293, 2012.

[29] R. Azzara, E. Carrera, M. Filippi, and A. Pagani. Time response stress analysis of solid and reinforced thin-walled structures by component-wise models. *International Journal of Structural Stability and Dynamics*, page 2043010, 2020.

[30] A. Pagani, R. Augello, and E. Carrera. Frequency and mode change in the large deflection and post-buckling of compact and thin-walled beams. *Journal of Sound and Vibration*, 432:88–104, 2018.

[31] A. Pagani, R. Azzara, R. Augello, E. Carrera, and B. Wu. Accurate through-the-thickness stress distributions in thin-walled metallic structures subjected to large displacements and large rotations. *Vietnam Journal of Mechanics*, 42(3):239–254, 2020.

[32] E. Carrera, A. Pagani, R. Azzara, and R. Augello. Vibration of metallic and composite shells in geometrical nonlinear equilibrium states. *Thin-Walled Structures*, 157:107131, 2020.

[33] F. Miglioretti, E. Carrera, and M. Petrolo. Variable kinematic beam elements for electromechanical analysis. *Smart Structures and Systems*, 13(4):517–546, 2014.

[34] E. Carrera, A. Pagani, R. Augello, and B. Wu. Popular benchmarks of nonlinear shell analysis solved by 1D and 2D CUF-based finite elements. *Mechanics of Advanced Materials and Structures*, pages 1–12, 2020.

[35] B. Wu, A. Pagani, W.Q. Chen, and E. Carrera. Geometrically nonlinear refined shell theories by carrera unified formulation. *Mechanics of Advanced Materials and Structures*, pages 1–21, 2019.

[36] M.A. Crisfield. An arc-length method including line searches and accelerations. *International Journal for Numerical Methods in Engineering*, 19(9):1269–1289, 1983.

[37] E. Carrera. A study on arc-length-type methods and their operation failures illustrated by a simple model. *Computers & Structures*, 50(2):217–229, 1994.

[38] E. Carrera, R. Azzara, E. Daneshkhah, A. Pagani, and B. Wu. Buckling and post-buckling of anisotropic flat panels subjected to axial and shear in-plane loadings accounting for classical and refined structural and nonlinear theories. *International Journal of Non-Linear Mechanics*, 133:103716, 2021.